Supporting Information for
Explosively launched spores of ascomycete fungi have drag minimizing shapes

Marcus Roper*,[1,2] Rachel Pepper,[3] Michael P. Brenner,[1] and Anne Pringle[2]

[1]*School of Engineering and Applied Sciences*

[2]*Department of Organismic and Evolutionary Biology*

[3]*Department of Physics, Harvard University, Cambridge, MA 02138*

Abstract

This document includes the following Supplementary Methods and Figures for the paper: "Explosively launched spores of ascomycete fungi have drag minimizing shapes":

I Interpolation of drag-minimizing shapes to arbitrary Reynolds numbers (Fig. S1).

II Discussion of the mechanics of spore flight, including the possible effect of friction within the ascus (Fig S2).

III List of ascomycete species included in our analysis (Fig S3).

IV Measurement of force of selection in the family Pertusariaceae (Fig S4).

* To whom correspondence should be addressed. E-mail: mroper@seas.harvard.edu

I. INTERPOLATION OF DRAG-MINIMIZING SHAPES

Computation of exact drag minimizing shapes using our gradient-descent algorithm (see Methods and Materials) is computationally expensive. For this reason, we interpolate from the aspect ratio and drag data for exact optimal shapes at a small set of values of $\mathcal{R}e$ to intermediate values of $\mathcal{R}e$, by approximating the minimum-drag body by the least-drag *spindle* formed by rotating the arc of a circle around the associated chord, and carrying out a single parameter search over chord to width ratios to find the spindle shape of minimum drag. Figures S1A and B show, respectively, the interpolation of the aspect ratio and drag of the optimal shapes between four exactly determined drag minimizing shapes (for $\mathcal{R}e = 0.1$, 1, 5, 10) by these spindles.

Since real spores do not have pointed apices, it is more appropriate to compare the shapes of real spores with least-drag ellipsoids. The aspect ratio of least-drag ellipsoids is systematically less than that of the exact drag minimizing shape (Fig. S1A), but the difference in drag is very small (Fig. S1B).

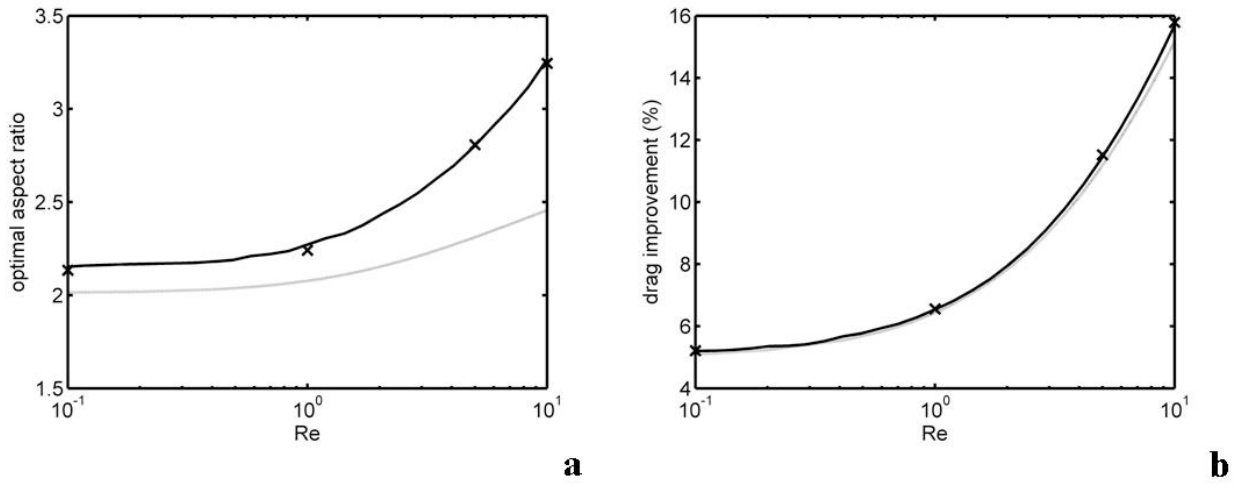

FIG. S1: Numerical calculation of drag minimizing shapes. **A** Interpolation of optimal aspect ratio between exact values (×) for $\mathcal{R}e = 0.1$, 1, 5, 10 using least-drag spindles (—). Least-drag spindles approximate the drag-minimizing shape as a segment of a circle revolved around its chord. Least-drag ellipsoids (—) lack fore and aft apices and have significantly smaller aspect ratios than the exact drag-minimizing shapes. **B** Variation of drag with $\mathcal{R}e$. The best spindles have drags very close to the minimum realizable drag at $\mathcal{R}e = 0.1$, 1, 5, 10. The key to symbols is identical to panel A. To compare the influence of body shape upon drag at different speeds, we plot drag improvement (% reduction in drag for an optimal shape compared to a sphere of the same volume). Although the aspect ratios of least-drag ellipsoids depart significantly from the aspect ratios of the exact drag minimizing shapes, the best ellipsoids come very close to the minimum possible drag for their size.

II. MECHANICS OF SPORE EJECTION AND FLIGHT

In this session we introduce three modeling assumptions that are made to find optimal spore shapes:

(i) Singly ejected unappendaged spores travel with fixed orientation in flight, and do not carry significant amounts of ascus fluid with them.

(ii) Spore shapes are not selected to maximize the speed of launch by minimizing frictional losses within the ascus.

(iii) The speed for which optimal spore shapes are selected is identified with the speed of launch.

(i) We expect spores to travel with a fixed orientation in flight, because in order to leave the ascus the spores pass through a narrow aperture. This aperture takes the form of a thickened ring of tissue in inoperculate fungi, or a narrow chimney set beneath a lid in suboperculate fungi, and is likely to fix the initial alignment of the spore, acting somewhat like the barrel of a mortar. Fluid dynamical instabilities that cause large projectiles such as thrown American footballs to tumble in flight are suppressed in this range of projectile speeds and sizes. We also assume that passing through the aperture separates spores both from each other, and from the epiplasm that fills the inflated ascus, so that spores are quite clean on leaving the ascus [3]. Although our high speed imaging does not provide sufficient resolution to confirm either of these assumptions, evidence for both is supplied by the frequency with which spores land long-axis in the direction of travel (indicating that they have not tumbled in flight) and well separated from droplets of ascus fluid, as can be seen in Figure S2**A**, taken from [6].

(ii) The spore may experience significant friction from the ascus walls when it passes through the aperture. This leads to considerable reduction in launch speed from the values expected from estimates of the over-pressure within the ascus (i.e. from (1)), and may cause the launch speed to depend upon spore shape. In fact it has been speculated that the shapes of forcibly ejected spores may be adapted to ensure the largest possible velocity of ejection [3], rather than for the minimization of drag in flight as we have hypothesized. Although such a constraint would also produce systematic differences of shape between ejected and non-ejected spores, we would expect it to produce selection for oblate, rather than prolate,

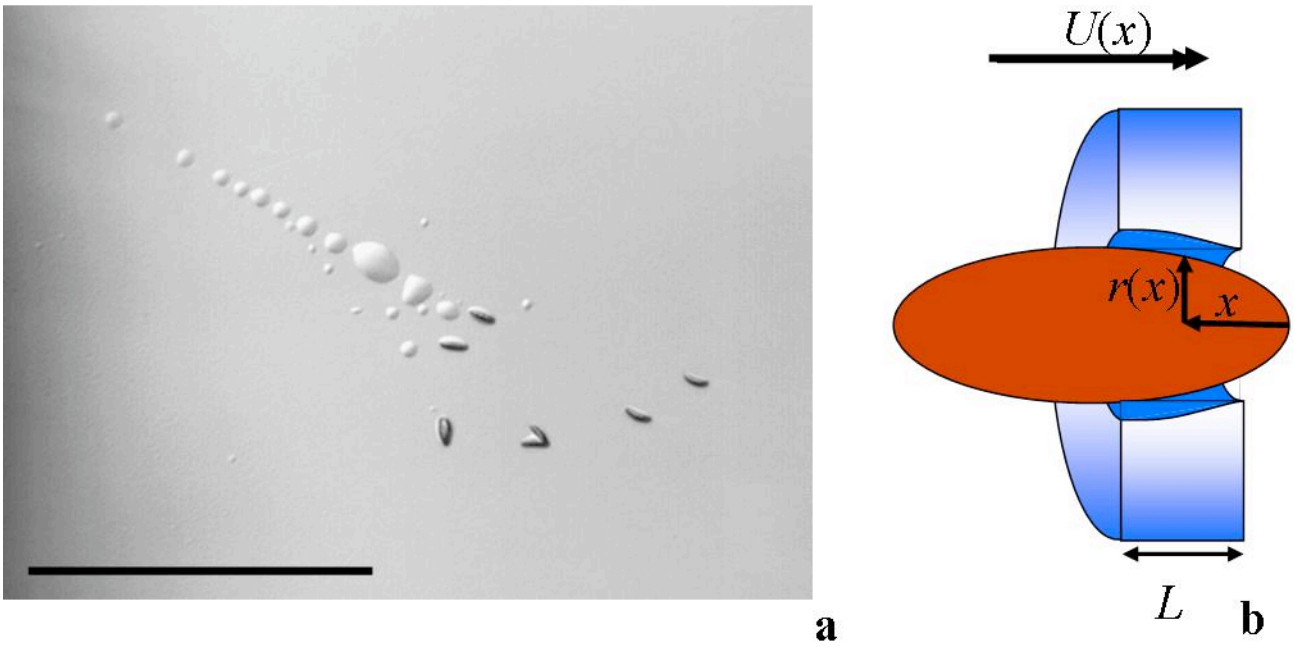

FIG. S2: **A** Spore print from a single ascus of the Sordariomycete species *Gibberella zeae*. The originating perithecium (outside of the image) lies to the upper left of the figure. Spores are clean of ascus sap, and point in the direction of travel. Scale bar: 100 μm. Reprinted with permission from Mycologia (ref. 7) (© 2002 The Mycological Society of America). **B** Sketch of a simple model for the effect of ascus friction upon launch speed. The friction on the spore is strongest in a thin lubricated layer of length L separating the spore and aperture walls.

spore shapes, as can be seen in a simple model of the process by which the spore is accelerated by turgor pressure within the ascus (Fig. S2B).

Consider a spore that is accelerated by a turgor pressure Δp, and experiences wall-friction from the aperture, which has length L and is sufficiently elastic to conform to the spore wall along the entire of this length. Denote by x the length of spore that has emerged from the ascus and assume that the greatest source of resistance to spore motion comes from the thin layer of fluid intercalated between the spore and aperture walls. We assume that this fluid layer has some constant thickness h which is maintained, for instance, either by elastohydrodynamic or electrostatic forces or by rigid decorations upon the spore surface. When moving through the aperture at speed U, the spore therefore encounters a lubrication drag of $2\pi\eta_s r(x)U/h$, where r is the local spore radius at the point of contact with the walls

of the aperture and η_s is the viscosity of the ascus sap. A force balance upon the spore then gives:

$$mU\frac{dU}{dx} = \pi r(x)^2 \Delta p - \frac{2\pi\eta r(x)U(x)}{h} \ , \tag{S1}$$

where the left hand side represents the inertia of the spore (we write m for the mass of the spore), and the right hand side the pressure and friction forces. For an ellipsoidal spore with length 2ℓ and width $2w$, $r(x) = (w/\ell)\sqrt{x(2\ell - x)}$ and we may rewrite the dynamical equation (S1) by scaling x by ℓ and the velocity of the spore by the launch speed in the absence of retardative force, $(8\pi w^2 \ell \Delta p/3m)^{1/2}$, to obtain:

$$U\frac{dU}{dx} = \frac{3}{8}x(2-x) - F\sqrt{x(2-x)}U \tag{S2}$$

where the F is the dimensionless strength of the friction force acting upon the spore:

$$F \equiv \sqrt{\frac{3\pi\ell\eta_s^2 L^2}{2m\Delta p h^2}} \ . \tag{S3}$$

$F \to 0$ corresponds to very weak wall friction. Accurate determination of the parameter F would require measurement of the thickness of the lubrication layer, h. Assuming a lubrication layer of thickness $0.1\,\mu$m, then for *Sordaria fimicola* ($\ell = 11\,\mu$m, $w = 7.5\,\mu$m, $L \approx 1\mu m$ [1, 5]) in water ($\eta_s = 10^{-3}\,$Pa s), we estimate that $F = 0.08$. Note however that the drag retardation due to friction can be made arbitrarily small if $\ell \to 0$: thus if spore volume is prescribed then maximizing the speed of launch favors highly oblate spores, which minimize the duration of contact with the walls of the aperture.

Our phylogenetic survey provides no evidence of forcibly ejected oblate spores, signalling that, in this form at least, launch speed maximization has not significantly contributed to the evolution of spore shape.

(iii) An additional assumption is our identification of the optimal speed of the spore with the speed of launch. The speed of an spore ejected into perfectly still air decreases quickly after launch, from the launch velocity U_0, which we know to be on the order of $\mathrm{m\,s^{-1}}$ to the speed of its steady sedimentation, which is typically just $\mathrm{mm\,s^{-1}}$. Under such circumstances, most of the distance traveled by the spore is covered during the very early stages of its motion [8], as can be seen most transparently for projectiles with $\mathcal{R}e < 1$, for which application of Eq.(2) gives that the distance traveled by a spore in any interval of time is directly proportional to the decrement in its velocity over that interval. In such cases, the

distance averaged velocity of the spore over the entire trajectory of the spore is just half of its launch speed. Note moreover that although the speed of the spore decreases asymptotically linearly with distance, the characters of the optimal spore shape vary much more slowly (apparently logarithmically) with the speed or size of the spore. Thus comparing real with optimal spores does not require precise knowledge of the speed of the spore or identification of the point in the spore trajectory for which range is optimized.

III. LIST OF RETAINED AND EXCLUDED SPECIES

The following criteria were used to exclude species from our analysis of forcibly ejected spore shapes. Letter codes are used to annotate a tree diagram of the retained and excluded species in Fig. S3.

- Fungi with no known sexual state (A) or not producing ascus-like spore sacs (T), including the Saccharomycotina, most of the Taphrinamycotina, and many Lichenous species.

- Ascus-producing species that do not explosively eject their spores (E), including the Eurotiomycetes and marine species of Sordariomycete.

- Species in which spores are not singly ejected (P). Since spore ejection has been directly observed in only a small number of species, and ascus ultra-structure recorded only in a small fraction of type descriptions, we have included in this list all polysporous species, including all Acarosporomycetidae.

- Ballistic species with appendages (Ap) or mucilaginous sheathes (Sh) spores, since such appendages are known to promote clumping of spores into single masses [4].

- Ballistic species with filiform spores (F). These spores are known to take up to 1 s to be ejected, and are likely to have launch velocities less than that of other members of the phylum [2]. We speculate that the great length of the spores (often in excess of 0.1 mm) allows them to physically span the boundary layer during the ejection process.

- Transversely septate (S) or muriform (M) species. Some spores of septate species, such as *Cordyceps*, *Acarosporina* and *Hypocrea citrina* are known to disarticulate into part spores either within the ascus or during ejection.

We also substituted the following species that were excluded according to one of the above criteria by closely related species that met all criteria:

- *Punctelia rudecta*, T, replaced by *P. perreticulata*.

- *Ionaspis lacustris*, Sh, replaced by *I. lavitra*.

- *Astrocystis cocoes*, Ap, replaced by *A. cepiformis*.

- *Hypocrea citrina*, S, replaced by *H. rufa*.

To ensure coverage of the entire range of observed spore sizes, the phylogeny was supplemented with the following large-spored species (binned by volumetric radius):

- 10–20 μm: *Chorioactis geaster*, *Pertusaria flavicans*, *P. chiodectonoides*, *P. geminipara*
- 20–30 μm: *Ochrolechia oregonensis*, *Pertusaria islandica*, *P. flavicunda*, *P. paratubiculifera*, *P. glomerata*, *P. pustulata*, *P. xanthostoma*,
- 30–40 μm: *Pertusaria macounii*, *P. plitania*, *P. multipuncta*, *P. opthalmiza*,
- 40–50 μm: *Pertusaria panyrga*, *P. albescens*, *P. velata*, *P. pseudocorallina*,
- 50–60 μm: *Pertusaria lactea*, *P. dactylina*, *P. bryontha*, *P. monogona*, *P. melanchora*,

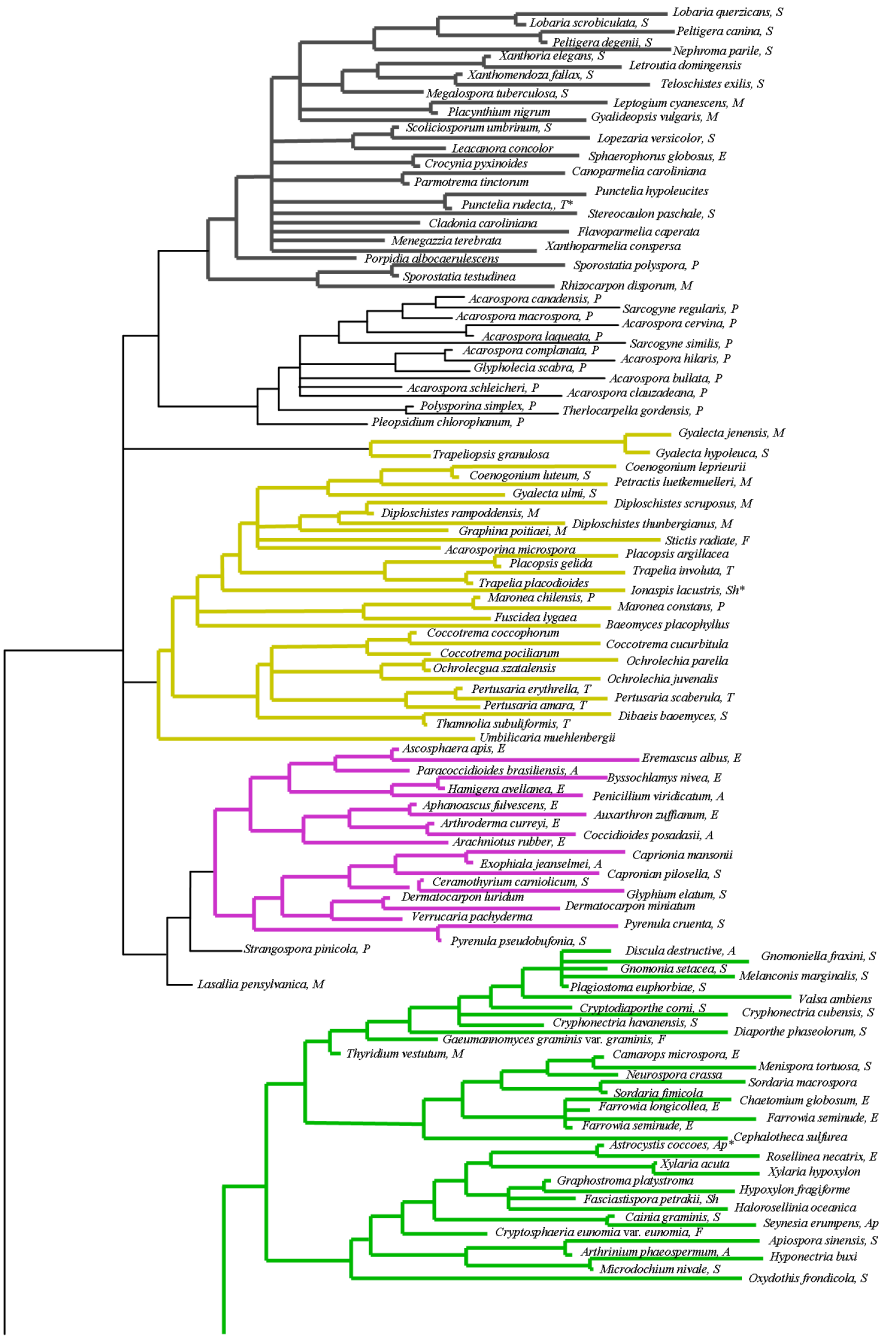
Lobaria querzicans, S
Lobaria scrobiculata, S
Peltigera canina, S
Peltigera degenii, S
Nephroma parile, S
Xanthoria elegans, S
Letrouitia domingensis
Xanthomendoza fallax, S
Teloschistes exilis, S
Megalospora tuberculosa, S
Leptogium cyanescens, M
Placynthium nigrum
Gyalideopsis vulgaris, M
Scoliciosporum umbrinum, S
Lopezaria versicolor, S
Leacanora concolor
Sphaerophorus globosus, E
Crocynia pyxinoides
Canoparmelia caroliniana
Parmotrema tinctorum
Punctelia hypoleucites
Punctelia rudecta,, T*
Stereocaulon paschale, S
Cladonia caroliniana
Flavoparmelia caperata
Menegazzia terebrata
Xanthoparmelia conspersa
Porpidia albocaerulescens
Sporostatia polyspora, P
Sporostatia testudinea
Rhizocarpon disporum, M
Acarospora canadensis, P
Sarcogyne regularis, P
Acarospora macrospora, P
Acarospora cervina, P
Acarospora laqueata, P
Sarcogyne similis, P
Acarospora complanata, P
Acarospora hilaris, P
Glypholecia scabra, P
Acarospora bullata, P
Acarospora schleicheri, P
Acarospora clauzadeana, P
Polysporina simplex, P
Therlocarpella gordensis, P
Pleopsidium chlorophanum, P
Gyalecta jenensis, M
Trapeliopsis granulosa
Gyalecta hypoleuca, S
Coenogonium luteum, S
Coenogonium leprieurii
Petractis luetkemuelleri, M
Gyalecta ulmi, S
Diploschistes scruposus, M
Diploschistes rampoddensis, M
Diploschistes thunbergianus, M
Graphina poitiaei, M
Stictis radiata, F
Acarosporina microspora
Placopsis argillacea
Placopsis gelida
Trapelia involuta, T
Trapelia placodioides
Ionaspis lacustris, Sh*
Maronea chilensis, P
Maronea constans, P
Fuscidea lygaea
Baeomyces placophyllus
Coccotrema coccophorum
Coccotrema cucurbitula
Coccotrema pociliarum
Ochrolechia parella
Ochrolecgua szatalensis
Ochrolechia juvenalis
Pertusaria erythrella, T
Pertusaria scabrula, T
Pertusaria amara, T
Dibaeis baoemyces, S
Thamnolia subuliformis, T
Umbilicaria muehlenbergii
Ascosphaera apis, E
Eremascus albus, E
Paracoccidioides brasiliensis, A
Byssochlamys nivea, E
Hamigera avellanea, E
Penicillium viridicatum, A
Aphanoascus fulvescens, E
Auxarthron zuffianum, E
Arthroderma curreyi, E
Coccidioides posadasii, A
Arachniotus rubber, E
Caprionia mansonii
Exophiala jeanselmei, A
Capronian pilosella, S
Ceramothyrium carniolicum, S
Glyphium elatum, S
Dermatocarpon luridum
Dermatocarpon miniatum
Verrucaria pachyderma
Pyrenula cruenta, S
Pyrenula pseudobufonia, S
Strangospora pinicola, P
Discula destructive, A
Gnomoniella fraxini, S
Gnomonia setacea, S
Melanconis marginalis, S
Plagiostoma euphorbiae, S
Valsa ambiens
Cryptodiaporthe corni, S
Cryphonectria cubensis, S
Cryphonectria havanensis, S
Diaporthe phaseolorum, S
Gaeumannomyces graminis var. graminis, F
Thyridium vestitum, M
Camarops microspora, E
Menispora tortuosa, S
Neurospora crassa
Sordaria macrospora
Sordaria fimicola
Chaetomium globosum, E
Farrowia longicollea, E
Farrowia seminude, E
Farrowia seminude, E
Cephalotheca sulfurea
Astrocystis coccoes, Ap*
Rosellinea necatrix, E
Xylaria acuta
Xylaria hypoxylon
Graphostroma platystroma
Hypoxylon fragiforme
Fasciastispora petrakii, Sh
Halorosellinia oceanica
Cainia graminis, S
Seynesia erumpens, Ap
Cryptosphaeria eunomia var. eunomia, F
Apiospora sinensis, S
Arthrinium phaeospermum, A
Hyponectria buxi
Microdochium nivale, S
Oxydothis frondicola, S
Lasallia pensylvanica, M

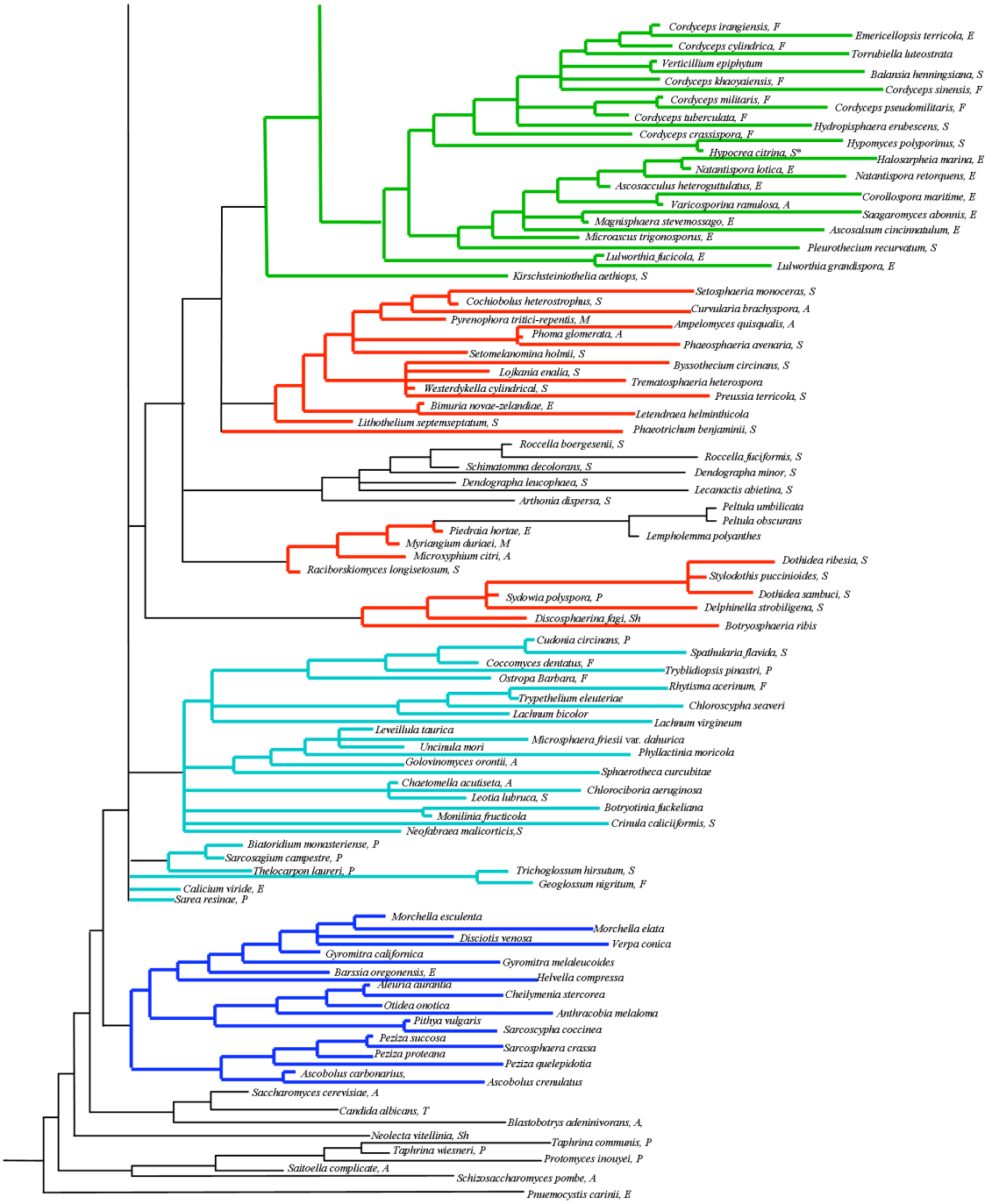

FIG. S3: Annotated tree of life for the Ascomycete fungi. Excluded species are marked with the rationale for exclusion (A,T,E,P,Ap,Sh,F,S,M). Substituted species are marked (*). The colour-coding of the classes is the same as for Figure 2a. Of 267 species from the original phylogeny, 73 species had forcible ejection and lacked additional adaptations so were used in our analysis. A further 4 species had adaptations but were substituted for by congeneric species lacking adaptations, and 25 additional large spored species were added.

IV. ESTIMATING THE FORCE OF SELECTION FOR DRAG MINIMIZING SHAPES IN THE FAMILY PERTUSARIACEAE

We compute the parameters representing the relative contributions from drift and selection to spore shape in the family Pertusariaceae by maximizing the probability of the invariant distribution of the process (3) producing the real species data. The small sample size (36 species) makes these this method of parameter estimation highly-sensitive to outlying data, but a good fit is achieved if we simply discard the small slender-spored species *Loxosporopsis corallifera*.

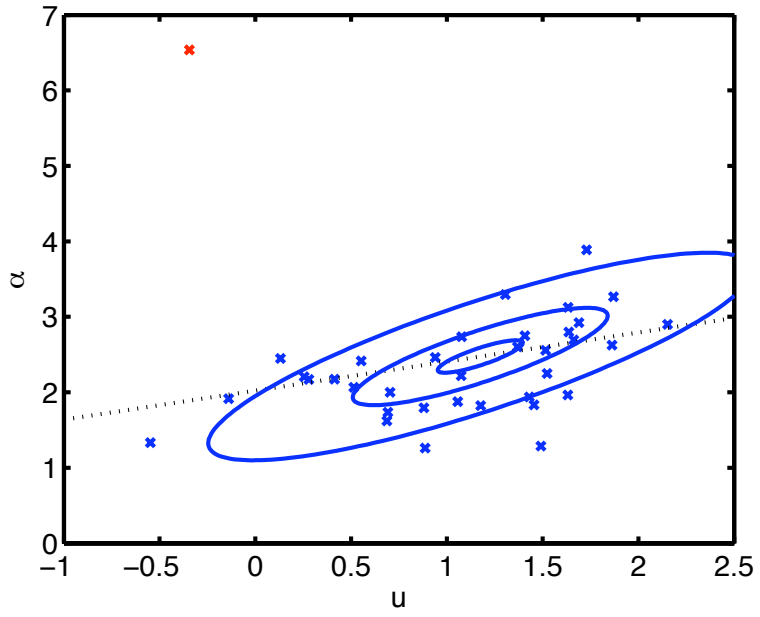

FIG. S4: Fitting the Pertusaria spore shape data (blue crosses) with the strong-selection model of Eq.(3). The blue ellipses are isoprobability contours. The dashed line gives the optimal spore aspect ratio. Because of the small sample size ($N = 36$), the maximum likelihood estimators of the model parameters are over-sensitive to unusual spore shapes, and one outlying species (*L. corallifera*, red cross) had to be discarded when fitting the model.

[1] R. W. G. Dennis, *British ascomycetes*, J. Cramer, 1981.

[2] C. Ingold, *Spore Discharge in Land Plants*, Oxford Univ. Press, 1939.

[3] ——, *Fungal spores : their liberation and dispersal*, Oxford Clarendon Press, 1971.

[4] E. Jones, *Form and function of fungal spore appendages*, Mycoscience, 47 (2006), pp. 167–183.

[5] F. Reeves, *The structure of the ascus apex in* Sordaria fimicola, Mycol., 63 (1971), pp. 204–212.

[6] F. Trail, I. Gaffoor, and S. Vogel, *Ejection mechanics and trajectory of the ascospores of* Gibberella zeae *(anamorph* Fuarium graminearum*)*, Fung. Gen. and Biol., 42 (2005), pp. 528–533.

[7] F. Trail, H. Xu, R. Loranger, and D. Gadoury, *Physiological and environmental aspects of ascospore discharge in* Gibberella zeae *(anamorph* Fusarium graminearum*)*, Mycol., 94 (2002), pp. 181–189.

[8] S. Vogel, *Living in a physical world II. The bio-ballistics of small projectiles*, J. Biosci., 30 (2005), pp. 167–175.